

UC Davis

UC Davis Previously Published Works

Title

Integration of plasma and CSF metabolomics with CSF proteomic reveals novel associations between lipid mediators and central nervous system vascular and energy metabolism.

Permalink

<https://escholarship.org/uc/item/1227b9rz>

Journal

Scientific Reports, 13(1)

Authors

Borkowski, Kamil
Seyfried, Nicholas
Arnold, Matthias
et al.

Publication Date

2023-08-23

DOI

10.1038/s41598-023-39737-8

Copyright Information

This work is made available under the terms of a Creative Commons Attribution License, available at <https://creativecommons.org/licenses/by/4.0/>

Peer reviewed



OPEN

Integration of plasma and CSF metabolomics with CSF proteomic reveals novel associations between lipid mediators and central nervous system vascular and energy metabolism

Kamil Borkowski¹✉, Nicholas T. Seyfried², Matthias Arnold^{3,4}, James J. Lah⁵, Allan I. Levey⁵, Chadwick M. Hales⁵, Eric B. Dammer², Colette Blach⁶, Gregory Louie⁴, Rima Kaddurah-Daouk^{4,7,8}✉ & John W. Newman^{1,9,10}

Integration of the omics data, including metabolomics and proteomics, provides a unique opportunity to search for new associations within metabolic disorders, including Alzheimer's disease. Using metabolomics, we have previously profiled oxylipins, endocannabinoids, bile acids, and steroids in 293 CSF and 202 matched plasma samples from AD cases and healthy controls and identified both central and peripheral markers of AD pathology within inflammation-regulating cytochrome p450/soluble epoxide hydrolase pathway. Additionally, using proteomics, we have identified five cerebrospinal fluid protein panels, involved in the regulation of energy metabolism, vasculature, myelin/oligodendrocyte, glia/inflammation, and synapses/neurons, affected in AD, and reflective of AD-related changes in the brain. In the current manuscript, using metabolomics-proteomics data integration, we describe new associations between peripheral and central lipid mediators, with the above-described CSF protein panels. Particularly strong associations were observed between cytochrome p450/soluble epoxide hydrolase metabolites, bile acids, and proteins involved in glycolysis, blood coagulation, and vascular inflammation and the regulators of extracellular matrix. Those metabolic associations were not observed at the gene-co-expression level in the central nervous system. In summary, this manuscript provides new information regarding Alzheimer's disease, linking both central and peripheral metabolism, and illustrates the necessity for the "omics" data integration to uncover associations beyond gene co-expression.

The development of multiple omics techniques provides a unique opportunity to probe different aspects of metabolic underpinnings of human disorders¹, including Alzheimer's disease (AD)^{2,3}. Metabolomics has been shown to be a useful tool in elucidating molecular manifestations of AD pathomechanisms^{4,5}. These include neuroinflammation, a core feature of AD⁶, where targeted metabolomic profiling of lipid mediators in matched plasma and cerebrospinal fluid (CSF) samples revealed evidence for a role of soluble epoxide hydrolase (sEH) and

¹West Coast Metabolomics Center, Genome Center, University of California Davis, Davis, CA 95616, USA. ²Department of Biochemistry, Emory University School of Medicine, Atlanta, GA 30322, USA. ³Institute of Computational Biology, Helmholtz Zentrum München-German Research Center for Environmental Health, Neuherberg, Germany. ⁴Department of Psychiatry and Behavioral Sciences, Duke University, Durham, NC 27708, USA. ⁵Department of Neurology, Emory University, Atlanta, GA 30329, USA. ⁶Duke Molecular Physiology Institute, Duke University, Durham, NC 27708, USA. ⁷Duke Institute for Brain Sciences, Duke University, Durham, NC 27708, USA. ⁸Department of Medicine, Duke University, Durham, NC 27708, USA. ⁹Western Human Nutrition Research Center, United States Department of Agriculture-Agriculture Research Service, Davis, CA 95616, USA. ¹⁰Department of Nutrition, University of California-Davis, Davis, CA 95616, USA. ✉email: kborkowski@ucdavis.edu; Rima.kaddurahdaouk@duke.edu

ethanolamides (a class of endocannabinoids) in AD-associated pathologies⁷. These metabolomic variables were distributed across the three classes of oxylipins, endocannabinoids (ECs) and bile acids (BAs). Oxylipins are bioactive oxygenated products of polyunsaturated fatty acids (PUFA) that exhibit both pro- and anti-inflammatory actions⁸. Oxylipin biosynthesis involves the actions of cyclooxygenases (COX), lipoxygenases (LOX), cytochrome P450 (CYP), epoxide hydrolases (EH), and reactive oxygen species, and encompass an array of chemical structures including prostaglandins and epoxides, as well as mono-, di- and tri-hydroxylated species^{8,9}. Endocannabinoids (ECs), named for the ability to activate the CB1 and CB2 cannabinoid receptors, are mainly fatty acid esters and amides that are implicated in regulation of both energy metabolism¹⁰ and inflammatory processes¹¹. However, the physiological impacts of ECs are not solely dependent on the CB1 and CB2 activation. ECs and like-substances also interact with the transient potential vanilloid receptor subfamily V member 1 (TRPV1), the G-protein-coupled receptor GPR55¹⁰ and the peroxisome proliferator-activated receptors (PPARs)¹². Each of these EC-sensitive receptors are highly expressed in the central nervous system (CNS)¹³. Primary BAs are generated by the liver and secreted into the gut to aid lipid digestion, where they are transformed by the gut microbiome into secondary BAs¹⁴. After reabsorption from the gut into the blood stream, BAs regulate energy homeostasis with different potency between primary and secondary species mediated through interactions with the farnesoid X receptor (FXR)¹⁵ and the G-protein-coupled bile acid receptor TGR5¹⁶. Although communication of these metabolites and proteins are well established, their interactions and regulation in the context of AD remain largely elusive.

The proteome and metabolome together are the end products in the biochemical “omics cascade”, provide a set of quantitative traits that respond to both genetic and environmental factors and constitute the building blocks of biochemical pathways. Because of their complementarity, integrating proteomic with metabolomics features has the potential to reveal molecular dependencies that go beyond genetic or transcriptional regulation. Previously, we described five functional protein panels in CSF, representing distinct physiological processes that are reflective of AD-associated changes in the brain¹⁷. These panels include a synaptic panel of neuronal proteins, a vascular panel of endothelial proteins involved in blood coagulation and interaction with extracellular matrix, a myelination panel of oligodendrocyte markers and cellular proliferation, a glial immunity panel of microglia and astrocyte markers and a metabolic panel of proteins involved in energy regulation and storage (i.e. glycolysis).

Since lipid mediators are the key regulators of inflammation among an array of other physiological processes, characterization of how specific peripheral and CSF lipid mediators interact and aggregate with the described functional protein domains in the context of neuroinflammatory processes in AD has the potential to enhance our mechanistic understanding of disease pathology. Alzheimer’s disease metabolomics consortium (ADMC) is a part of accelerated medicine partnership initiative (AMP) and provides a vast repository of the omics data collected from multiple AD-related cohorts. In the current study, we consequently used ADCM repository of a matched dataset of CSF proteomic panels with CSF and plasma lipid mediator panels in a cohort of participants with and without AD, to probe interactions between these neighboring levels of the omics cascade. Additionally, the newly discovered associations were tested using the cerebral gene co-expression network, to see whether those associations exist uniquely on protein-metabolite level. We report new interactions between peripheral and central CYP/sEH and BAs metabolism and energy and vascular metabolism in the CNS, describing new connection of inflammation and liver/gut microbiome metabolism and AD.

Materials and methods

Subjects. This manuscript contains a secondary analysis of previously described studies^{7,17} with demographics previously summarized⁷. All participants from whom plasma and CSF samples were collected provided informed consent under protocols approved by the Institutional Review Board at Emory University. All protocols were reviewed and approved by the Emory University Institutional Review Board. Cohorts included the Emory Healthy Brain Study (IRB00080300), Cognitive Neurology Research (IRB00078273), and Memory @ Emory (IRB00079069). All patients received standardized cognitive assessments (including Montreal Cognitive Assessment (MoCA)) in the Emory Cognitive Neurology clinic, the ADRC and affiliated Emory Healthy Brain Study (EHBS)¹⁸. All diagnostic data were supplied by the ADRC and the Emory Cognitive Neurology Program. CSF was collected by lumbar puncture and banked according to 2014 ADC/NIA best practices guidelines. All CSF samples collected from research participants in the ADRC, Emory Healthy Brain Study, and Cognitive Neurology clinic were assayed for total Tau, phosphorylated Tau and AB42 using the INNO-BIA AlzBio3 Luminex assay at AKESOgen (Peachtree Corners, GA). AD cases and healthy individuals were defined using established biomarker cutoff criteria for AD for each assay platform^{19,20}. In total, this analysis utilized data from 202 fasting plasma samples (60 AD cases and 142 healthy controls) and 293 CSF samples (151 AD cases and 142 healthy controls). Two hundred two plasma and CSF samples were matched and collected at the same day. General study design is provided in the Fig. S1.

Quantification of lipid mediators. Lipid mediators from multiple functional domains and metabolite classes were quantified in 202 plasma and 293 CSF using internal standard methodologies and liquid chromatography tandem mass spectrometry (LC–MS/MS) as reported previously^{7,21}. Briefly, concentrations of non-esterified PUFA, oxylipins, endocannabinoids, a suite of conjugated and unconjugated BAs, and a series of glucocorticoids, progestins and testosterone were quantified by liquid chromatography tandem mass spectrometry (LC–MS/MS) after protein precipitation in the presence of deuterated metabolite analogs (i.e. analytical surrogates). Quality control measures included case/control randomization, and the analysis of batch blanks, pooled matrix replicates and NIST Standard Reference Material 1950—Metabolites in Human Plasma (Sigma-Aldrich, St Louis, MO) (two per experimental batch). Extracted samples were re-randomized within batch for acquisition, with method blanks and reference materials and calibration solutions scattered regularly throughout the

set. The quality control process included removal of data with signal to noise ratio < 3 and exclusion of variables with $> 75\%$ of missing data. Additionally, the outliers were removed using the robust Huber M test and missing data were imputed using multivariate normal imputation. The data were transformed to normal, scaled and centered using Johnson's transformation.

Quantitative CSF proteomics. Previously published tandem mass tag (TMT) RAW data of LC–MS/MS tryptic peptide digests of whole CSF from 293 individuals were analyzed using the Proteome Discoverer Suite (version 2.3, ThermoFisher Scientific)^{17,22}. Briefly, MS/MS spectra were searched against the UniProtKB human proteome database (downloaded April 2015 with 90,411 total sequences). The Sequest HT search engine was used to search the RAW files, with search parameters specified as follows: fully tryptic specificity, maximum of two missed cleavages, minimum peptide length of 6, fixed modifications for TMT tags on lysine residues and peptide N-termini (+ 229.162932 Da) and carbamidomethylation of cysteine residues (+ 57.02146 Da), variable modifications for oxidation of methionine residues (+ 15.99492 Da), serine, threonine and tyrosine phosphorylation (+ 79.966 Da) and deamidation of asparagine and glutamine (+ 0.984 Da), precursor mass tolerance of 20 ppm, and a fragment mass tolerance of 0.6 Da. Percolator was used to filter PSMs and peptides to an FDR of less than 1%. Following spectral assignment, peptides were assembled into proteins and were further filtered based on the combined probabilities of their constituent peptides to a final FDR of 1%. In cases of redundancy, shared peptides were assigned to the protein sequence in adherence with the principles of parsimony as implemented in the Proteome Discoverer software. Reporter ions were quantified using an integration tolerance of 20 ppm with the most confident centroid setting. We have previously described identification of 46 CSF proteins that corresponds to AD-related changes in brain¹⁷. Five of those proteins were excluded from the analysis in this manuscript due to $> 25\%$ of missing variables. Remaining 41 proteins were converted into the z-scores and subsequently into residuals of age, sex, race and ApoE genotype effects, to account for confounders. Protein classification according to GO annotations as well as more in-depth functional classification based on the current literature is presented in the Table S1.

Metabolite–protein interactions. To explore connections between CNS metabolites and protein expression, we examined correlations between 41 CSF proteins affected by AD with 40 CSF lipid mediators and important metabolite ratios. The metabolic ratios were derived to: (a) emphasize enzymatic activity or biological process by calculating product to substrate ratios, for example fatty acid vicinal diols over corresponding fatty acid epoxides for sEH activity, or secondary BAs over the corresponding primary BAs for metagenome activity; (b) to emphasize alternative metabolic pathways, for example the ratio of 11,12-DiHETrE over 14,15-DiHETrE could be indicative of change in soluble epoxide hydrolase to microsomal epoxide hydrolase activity, or the ratio of CA to CDCA or their further metabolites could be an indication of the acidic or neutral BAs synthesis pathway. Associations were assessed using Spearman's rank order correlation to account for non-linear associations, using JMP software (SAS institute, Cary, NC). Similarly, to investigate associations between plasma metabolites and CSF proteins, we calculated correlations between the 41 CSF proteins with 93 detected plasma metabolites, including oxylipins, endocannabinoids and fatty acids and their important ratios. Multiple comparison control was accomplished with the false discovery rate (FDR) correction method of Benjamini and Hochberg with a $q = 0.2$ ²³ to allow for 20% of expected proportion of false positives. These analyses were performed separately for participants with and without diagnosed AD, allowing an investigation of the effect of the disease on those associations. Additionally, full factorial linear model was used to test for the metabolite \times disease state interaction. Prior to analysis, we converted all variables into residuals of age, sex, race and ApoE genotype effects, to account for confounders. Additionally, we used variable clustering to further illustrate the associations between CSF and plasma metabolites and CSF proteins. To this end, we used an implementation of the PCA based VARCLUS algorithm (JMP, SAS institute, Cary, NC) to cluster metabolites and proteins showing the greatest number and strongest interactions, such as sEH metabolites and proteins highlighted in Figs. S1 and S3.

Cerebral gene co-expression analysis. Potential interaction on a gene expression level between CSF proteins and enzymes involved in oxylipins and fatty acids biology were explored using data from The Genotype-Tissue Expression (GTEx) Project²⁴ available through the inetmodels.com platform. Network parameters: tissue—brain cerebrum; tissue type—normal tissue; maximal number of connections pre gene—25. Additional co-expression data from seven brain regions²⁵ and genetic associations between input proteins and AD were obtained using the AD Atlas²⁶. The list of proteins submitted to the network analyses is provided in Table S2.

Partial least square discriminant analysis. Partial least square discriminant analysis (PLS-DA) was used to investigate the relationship between CSF proteins in discrimination between AD cases and healthy controls, visualizing their multivariate and covariate structure. The PLS-DA model was built using the nonlinear iterative partial least squares algorithm with leave one out cross-validation and included all 41 CSF proteins. For the sake of clarity, we only displayed variables with a variable importance in projection (VIP) score > 1 on the loading plot (Fig. 5A).

Results

CSF sEH metabolites and PUFA show associations with CSF proteins regulating energy metabolism, vascular function and ECM interaction. Of the 41 tested proteins, 23 showed more than two significant associations with CSF metabolites (Fig. S2). According to GO classification, 12 of those 23 proteins belong to the vascular panel, five to metabolism panel, three were related to myelin/oligodendrocyte biology, two to synaptic/neuronal function and one to glia/inflammation¹⁷. Additionally, investigation beyond

GO annotations revealed five of those proteins to be involved in glycolysis, four in blood coagulation and six in interaction with the extracellular matrix (ECM) (protein functionality is summarized in the Table S1. Spearman's ρ and correlation p-values for all associations are presented in Table S3).

Soluble epoxide hydrolase (sEH) metabolites and long chain polyunsaturated fatty acids (PUFA) showed the greatest number of associations. To provide a general picture, metabolites and proteins that showed the greatest number of associations were collapsed into cluster components using variable clustering. The correlation matrix of those clusters of CSF metabolites and CSF proteins is shown in the Fig. 1. CSF metabolites formed two clusters: containing sEH metabolites of arachidonic acid (AA) (11,12-DiHETrE and 14,15-DiHETrE) and docosahexaenoic acid (DHA)-Derived 19,20-DiHDoPE, with the R^2 of those metabolites with its own cluster equal 0.87, 0.86 and 0.68 respectively; containing long chain PUFAs, including DHA, eicosapentaenoic acid (EPA) and AA, with the R^2 with its own cluster equal 0.87, 0.80 and 0.77 respectively. CSF proteins formed 3 clusters: Cluster 1, represented by vascular proteins F2, AMBP and VTN; Cluster 2 represented by proteins involved in energy metabolism (PKM and ALDOA) and cell proliferation (PEBP1); and Cluster 3 containing the two glycolytic enzymes ENO2 and ALDOC, as well as COL61A, which is involved in ECM synthesis (cluster members and their correlation within each cluster component are described in the Table S5).

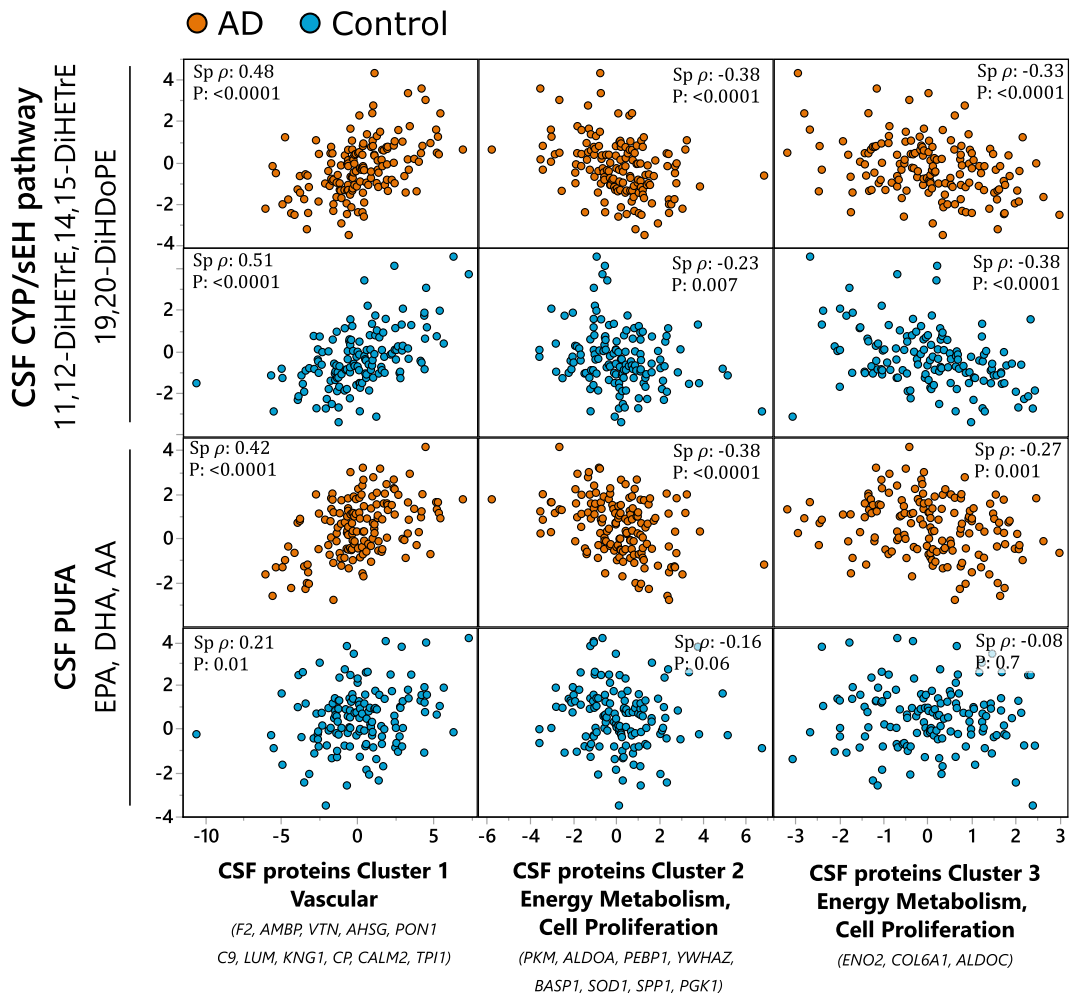


Figure 1. CSF sEH metabolite and PUFAs associations with AD-implicated CSF protein clusters. Most pronounced associations collapsed into variable cluster components, with the indicated Spearman's rank order correlation statistics, including Spearman's ρ and p-value. The sEH metabolites cluster was created from 11,12-DiHETrE, 14,15-DiHETrE and 19,20-DiHDoPE and the PUFA cluster from EPA, DHA and AA. CSF proteins were organized into three clusters (Table S5): cluster 1—containing mostly vascular proteins, with F2, AMBP and VTN as most representative members with $R^2 > 0.8$; Cluster 2—containing proteins involved in energy metabolism and cell proliferation, with PKM, ALDOA and PEBP1 as most representative members with $R^2 > 0.7$; Cluster 3 containing glycolysis regulating ENO2 and cell proliferation regulating COL6A1 and glycolytic enzyme ALDOC. Analysis was performed separately for AD cases and healthy controls and the two groups are indicated on the graph by colors: blue—healthy control; orange—AD cases. N for AD cases = 151; healthy controls = 142.

In general, both sEH and PUFA clusters showed positive associations with CSF vascular protein cluster (cluster 1 with F2, AMBP and VTN as most representative proteins). Negative associations were observed between sEH and PUFA clusters and CSF proteins regulating energy metabolism and cell proliferation (cluster 2, with PKM, ALDOA and PEBP1 as most representative proteins and cluster 3 composed of ENO2, COL6A1 and ALDOC). For the sEH cluster, the observed associations were similar between AD and healthy controls, with Spearman's $\rho = 0.48, -0.38$ and -0.33 in AD cohort and $0.51, -0.23$ and -0.38 in the healthy control cohort, for the protein clusters 1, 2 and 3 respectively. No interaction with the disease state were detected between sEH metabolites and described CSF protein clusters in the full factorial linear model ($P_{\text{interaction}} = 0.75, 0.36$ and 0.64 for cluster 1, 2 and 3 respectively). On the other hand, the PUFA cluster showed strong associations only in the AD group, with Spearman's $\rho = 0.42, -0.38$ and -0.27 in AD cohort and $0.21, -0.16$ and -0.08 in the healthy control cohort, for the protein clusters 1, 2 and 3 respectively. The $P_{\text{interaction}}$ in the full factorial linear model were $0.045, 0.019$ and 0.084 for the CSF protein clusters 1, 2 and 3 respectively).

Of note, each metabolite within the cluster independently manifested a similar pattern of associations with CSF proteins, showed in detail in the Fig. S2.

CSF bile acid associations with CSF proteins. Conjugated derivatives of chenodeoxycholic acid (CDCA) and deoxycholic acid (DCA) showed the greatest number of associations with CSF proteins (Fig. S3 and Table S3). To provide a general picture, bile acids that showed the greatest number of associations were collapsed into cluster components using variable clustering. The correlation matrix of those clusters of CSF bile acids with previously described CSF protein clusters is shown in the Fig. 2. CSF bile acids formed two clusters: containing CDCA conjugates, including GCDCA and TCDCA, with the R^2 with the cluster equal 0.88 each; containing DCA conjugates, including GDCA and TDCA, with the R^2 with the cluster equal 0.88 each. Both bile acids clusters demonstrated similar pattern of correlations with CSF proteins with the positive association with CSF vascular protein cluster and negative association with CSF proteins regulating energy metabolism and cell proliferation (clusters 2 and 3). No significant interaction with the disease state were detected between bile acid clusters and described CSF protein clusters in the full factorial linear model ($P_{\text{interaction}} = 0.08, 0.52$ and 0.5 for CDCA conjugates and $0.33, 0.09$ and 0.97 for DCA conjugates and CSF protein clusters 1, 2 and 3 respectively). However, the association between DCA conjugates and CSF protein cluster 2 was not significant. For the CDCA conjugates, the Spearman's $\rho = 0.32, -0.25$ and -0.38 in AD cohort and $0.48, -0.28$ and -0.35 in the healthy control cohort, for the protein clusters 1, 2 and 3 respectively. For the DCA conjugates, the Spearman's $\rho = 0.41, -0.31$ and -0.3 in AD cohort and $0.33, -0.08$ and -0.29 in the healthy control cohort, for the protein clusters 1, 2 and 3 respectively. Of note, each bile acid within the cluster independently manifested a similar pattern of associations with CSF proteins, showed in detail in the Fig. S3.

Plasma CYP metabolism is associated with CSF proteins regulating energy metabolism, vascular function, and ECM interaction. Of 41 tested proteins, 23 showed more than two significant associations with plasma metabolites (Fig. S4). Ten of those proteins belong to vascular panel, four to the metabolism panel, five to the myelin/oligodendrocyte panel, three to synaptic/neuronal function panel and one to the glia/inflammation panel. Three of the proteins were involved in glycolysis, five in blood coagulation and five in interaction with ECM.

Of the metabolite classes investigated, the greatest number of associations were observed with cytochrome p450/sEH metabolites, PUFA, endocannabinoids, several hydroxy-fatty acids and prostaglandin D2 (PGD2). Individuals with and without diagnosed AD showed distinct metabolite-protein correlations. In AD cases, the strongest associations were observed between the CYP-derived LA epoxide 9(10)-EpOME, and included positive associations with glycolysis proteins, negative associations with blood coagulating proteins, and strong but mixed associations with ECM interaction proteins. Similarly, three of the five measured PUFAs, aLA, LA and AA showed positive associations with two glycolysis proteins (PGK1 and ALDOA) and negative associations with two ECM interaction protein (VTN and MFGE8). Inverse associations were seen with hydroxy fatty acids. The DHA-derived 14-HDoHE and AA-derived 8-HETE and the ratio of LA-derived 13-KODE/13-HEDE and PGD2 showed negative associations with glycolysis proteins and positive associations with blood coagulation proteins and ECM interaction protein. These associations were absent in healthy controls. Spearman's ρ and correlation p-values for all associations are presented in Table S6. To summarize and further demonstrate the relations between plasma CYP metabolism and CSF proteins, we analyzed associations between LA derived CYP metabolite—9(10)-EpOME and CSF protein using variable cluster components (Fig. 3). CSF proteins formed three clusters: Cluster 1 represented by vascular proteins F2, AMBP and VTN; Cluster 2 represented by proteins involved in energy metabolism (PKM and ALDOA) and cell proliferation (PEBP1); Cluster 3, containing PGK1 that is involved in energy metabolism, and SMOC1 and PPIA, which are involved in cell proliferation (individual cluster members and their correlation within each cluster components are described in the Table S5). The LA epoxide 9(10)-EpOME showed a strong negative association with Cluster 1 (vascular panel), and positive associations with Cluster 2 (cell proliferation and energy metabolism) only among AD cases, and no associations with Cluster 3 (glycolysis, cell proliferation) (Spearman's $\rho = -0.44, 0.47$ and 0.15 in AD cohort and $-0.1, 0.05$ and -0.06 in the healthy control cohort, for the protein clusters 1, 2 and 3 respectively). The $P_{\text{interaction}}$ in the full factorial linear model were $0.054, 0.0053$ and 0.17 for the CSF protein clusters 1, 2 and 3 respectively.

Plasma bile acid associations with CSF proteins. Of the 41 tested proteins, 15 showed more than two significant associations with plasma BAs (Fig. S5). Ten of those proteins belong to the vascular panel, two to the metabolism panel, one was related to the myelin/oligodendrocyte panel, and two to the glia/inflammation panel. Three of the proteins were involved in glycolysis, four in blood coagulation and six in interaction

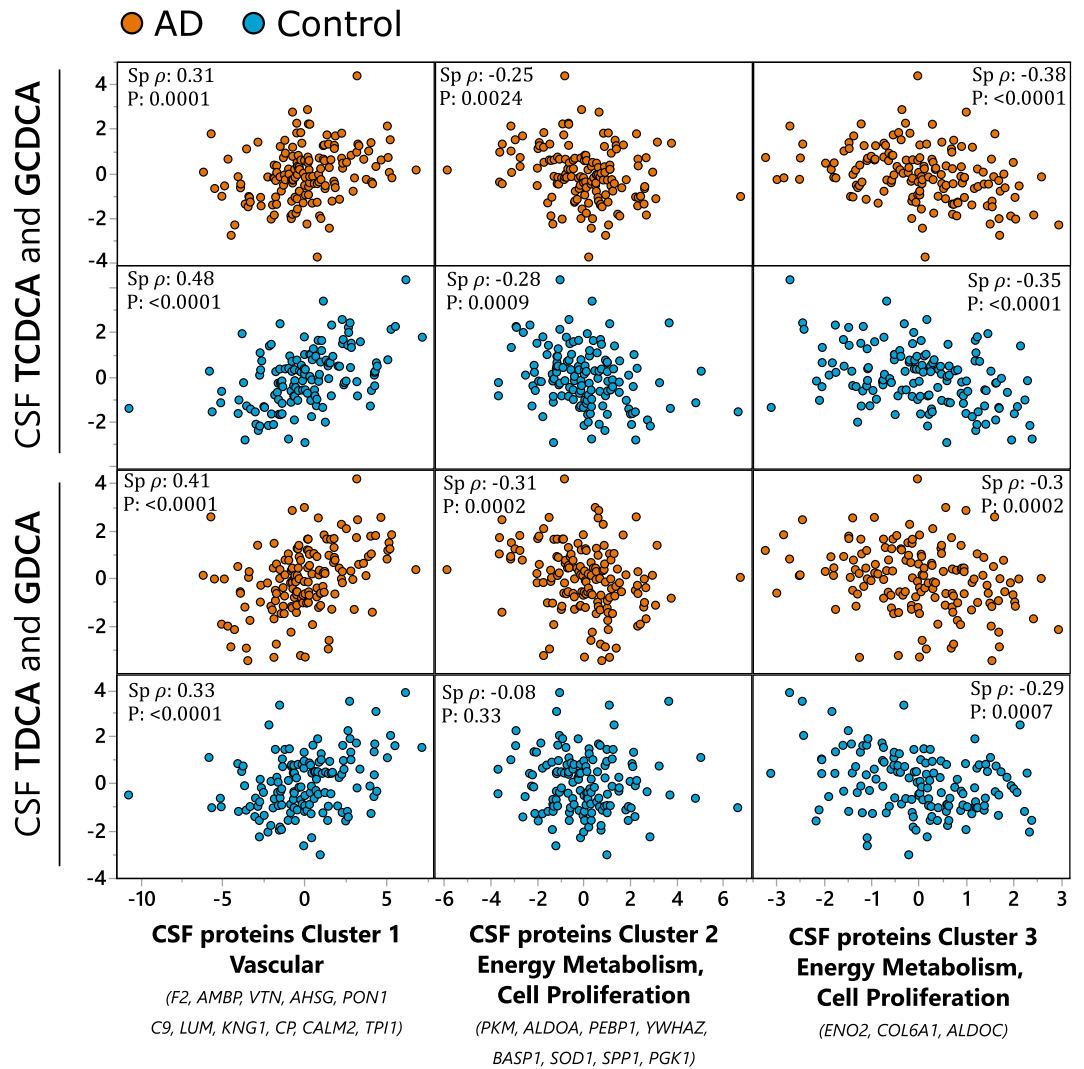


Figure 2. CSF bile acids associations with AD-implicated CSF protein clusters. Most pronounced associations collapsed into variable cluster components with the indicated Spearman's rank order correlation statistics, including Spearman's ρ and p-value. Two bile acids clusters were formed: one using GCDCA and TCDCa (upper two panels) and second using TDCA and GDCA (lower two panels). CSF proteins were organized into three clusters (Table S5): Cluster 1—containing mostly vascular proteins, with *F2*, *AMBP* and *VTN* as most representative members with $R^2 > 0.8$; Cluster 2—containing proteins involved in energy metabolism and cell proliferation, with *PKM*, *ALDOA* and *PEBP1* as most representative members with $R^2 > 0.7$; Cluster 3 containing glycolysis regulating *ENO2* and cell proliferation regulating *COL6A1* and glycolytic enzyme *ALDOC*. Analysis was performed separately for AD cases and healthy controls and the two groups are indicated on the graph by colors: blue—healthy control; orange—AD cases. N for AD cases = 151; healthy controls = 142.

with ECM. In AD cases, the greatest number of associations were formed with the specific BA ratios representing the relative activity of the classic and alternative BAs synthesis pathways, calculated using conjugated BAs: $(TCA + GCA + TDCA + GDCA) / (GUDCA + TUDCA + GLCA + TLCA + TCDCa + GCDCA)$, that showed negative associations with *ENO2* (Spearman's $\rho = -0.32$) and positive associations with proteins involved in blood coagulation and ECM interaction (*CP*, *KNG1*, *AMBP*, *PON1*, *LUM*, *SPP1*, *VNT* and *AHSG* with Spearman's $\rho = 0.29, 0.41, 0.5, 0.34, 0.35, 0.36, 0.29, 0.38$ and 0.47 respectively). Notably, only few of those associations were observed in healthy controls, however, significant disease state interactions were not observed in the linear full factorial model (Table S4). Spearman's ρ and correlation p-values for all associations are presented in Table S6.

Brain AD-related and CYP/sEH metabolism-related gene co-expression networks. Unlike BAs, lipid metabolism in the CNS is insulated from peripheral metabolism⁷. Therefore, using data from The Genotype-Tissue Expression (GTEx) Project²⁴ available through [inetmodels.com](https://www.inetmodels.com), we explored the co-expression of genes involved in identified lipid mediators and polyunsaturated fatty acid metabolism and proteins affected by AD. All AD-associated proteins presented in the Fig. S2 were submitted to the analysis using the cerebral brain region of healthy subjects as tissue (Fig. 4). Gene expression data was not available for members of BAs receptors,

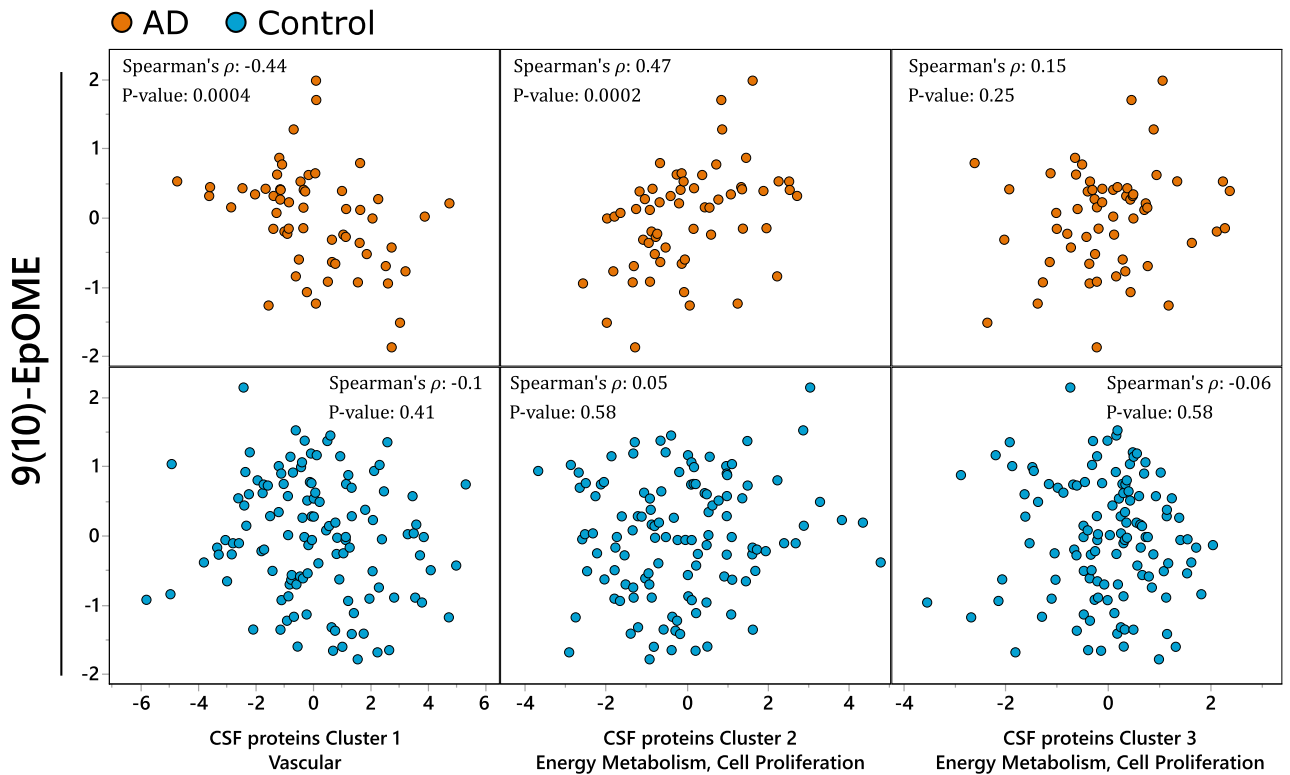


Figure 3. Plasma CYP associations with CSF proteome. Plasma CYP LA metabolite—9(10)-EpOME and CSF proteins collapsed into three cluster components (Table S5): Cluster 1—containing mostly vascular proteins, with F2, AMBP and VTN as most representative members with $R^2 > 0.7$; Cluster 2—containing proteins involved in energy metabolism and cell proliferation, with PKM, ALDOA and PEBP1 as most representative members with $R^2 > 0.7$; Cluster 3 containing glycolytic enzyme PGK1 and cell proliferation regulating SMOC1 and PPIA. Spearman's rank order correlation statistics, including Spearman's ρ and p-value are indicated for each correlation. Analysis was performed separately for AD cases and healthy controls due to significant difference in observed associations. N for AD cases = 60; healthy controls = 142.

including the farnesoid X receptor (FXR), pregnane X receptor (PXR), vitamin D receptor (VDR) and G protein-coupled bile acid receptor 1 (TGR5).

Of 23 AD-associated proteins (showing associations with CSF metabolites, described in the section "CSF sEH metabolites and PUFA show associations with CSF proteins regulating energy metabolism, vascular function and ECM interaction"), 12 were present in the GTEx database and all missing proteins belonged to the vascular panel. To interrogate polyunsaturated fatty acids metabolism, we selected genes involved in the PUFA epoxide/epoxide hydrolase pathway. Specific to epoxy fatty acid metabolism we included the only known CYP with PUFA epoxidase activity in the GTEx database, CYP2J2²⁷, the sEH (EPHX2) and the microsomal epoxide hydrolase (EPHX1), recently suggested to play parallel/complimentary roles in epoxy-PUFA degradation²⁸. We then extended this to include fatty acid metabolizing enzymes, including hormone sensitive lipase (LIPE) and fatty acid desaturase 2 (FADS2). We then sought to provide context with proteins involved at the intersection of AD and lipid metabolism. To this end, we included apolipoprotein E (ApoE), a critical apolipoprotein involved in PUFA and oxylipin trafficking with clear AD-associations²⁹ and TNF α Receptor Associated Factor 4 (TRAF4), an inflammatory cascade regulator upregulated in brains of AD cases³⁰ with expression levels reportedly associated with EPHX2 in cerebrum³¹. Generally, the CSF-AD protein panel formed a tight gene co-expression network distinct from that of lipid metabolizing proteins. Notably, in the lipid/oxylipin metabolism network, ApoE expression was closely associated with that of EPHX2 and ALDOC, while CYP2J2 expression was closely associated with EPHX1 and TRAF4 expression.

We further investigated potential gene co-expression of CSF proteins and above-described lipid mediators -regulating genes using AD Atlas²⁶ and seven brain regions. Strong associations were observed within investigated proteins, however no associations were observed between those proteins and lipid mediators enzymatic regulators. Additionally, genetic association ($p = 1 \times 10^{-13}$) was observed between EPHX2 gene and AD phenotype.

Vascular protein panel in CSF changes the dynamics of energy metabolism in AD. To further understand the relationship between different functional CSF protein panels and AD we implemented a partial least square discriminant analysis (PLS-DA) (Fig. 5). Out of 41 CSF proteins subjected to the analysis, 17 manifested variable importance in projection (VIP) scores > 1 . Generally, the model performed well with the $Q^2 = 0.48$ for two factors, achieving good separation between AD and control subjects. AD and control separation was

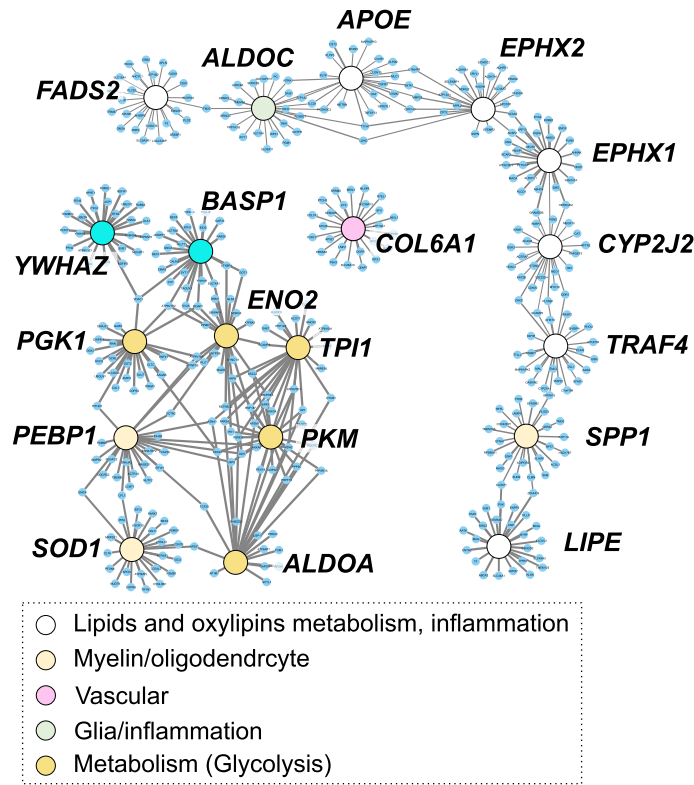


Figure 4. Cerebral gene co-expression network for AD-affected proteins and genes involved in oxylipins and lipids metabolism and inflammation. Nodes are colored according to gene annotation, analogical to Figure S2–S5. White nodes represent genes involved in: oxylipins metabolism like main isoform of cytochrome P450 epoxygenase (CYP2J2), soluble epoxide hydrolase (EPHX2) microsomal epoxide hydrolase (EPHX1); lipid metabolism including fatty acids desaturase 2 (FADS2), apolipoprotein E (ApoE), hormone sensitive lipase (LIPE); inflammation—TNF Receptor Associated Factor 4 (TRAF4).

driven by two functional groups of proteins (indicated by arrows in the Fig. 5A): (1) energy metabolism and cell proliferation proteins (i.e. key glycolytic proteins ALDOA, PKM and cell proliferation regulating PEBP1, all highly correlated in CSF ($r^2 > 0.8$); (2) vascular panel proteins, involved in blood coagulation and inflammation (VTN, F2, KNG1, AMBP). Noticeable, vascular proteins were not directly discriminating between AD and controls, but rather served as a covariate for the energy metabolism and cell proliferation proteins. To further illustrate the relationship between energy metabolism and vascular function in the context of AD, vascular proteins were converted into a composite score, and subjects were divided into quartiles of the vascular proteins composite score (Fig. 5B, left panel). Next, we showed that the level of energy metabolism and cell proliferation proteins (converted into one composite score) is higher in the subjects with low levels of vascular proteins composite score (Fig. 5B, right panel).

Discussion

In the current manuscript, we have explored associations between peripheral and CSF lipid mediators and bile acid metabolism with an AD-affected CSF proteome. Our analysis identified, to our knowledge for the first time, associations between CYP/sEH-derived metabolites, PUFAs and BAs with proteins involved in energy metabolism and cell proliferation, blood coagulation and vascular inflammation and ECM regulation in the CNS. Notably, both plasma and CSF members of CYP/SEH pathway, and CSF fatty acids, and BAs form strong associations with CSF proteins reflective of AD-related changes in brain¹⁷. Together, these results show the value of the integration of terminal omics data through utilization of previously published datasets.

Accumulating evidence suggests involvement of lipid mediators in AD pathology. Particularly, several oxylipins of the acute inflammation pathway are elevated in AD^{32,33} and compounds which stimulate inflammatory resolution have been suggested for AD treatment³⁴. Specific changes in BAs metabolism, including a decrease in primary and an increase in secondary metabolites were also observed in AD subjects³⁵ and alterations in bile acid metabolizing enzymes were reported in the AD afflicted brain³⁶. Notably, some BAs and some steroids manifest neuroprotective functions through activation of steroid receptors³⁷.

The involvement of the brain sEH pathway in AD was previously suggested by us⁷ and others^{38,39}. CYP/sEH pathway is known to regulate vascular tone⁴⁰ and inflammation⁴¹ in the periphery, and the current manuscript further implicates this pathway in regulation of the CNS vascular system, including vascular inflammation and potentially vascular dysfunction in the CNS, a process attributed to AD pathology⁴². Additionally, protein associations with sEH metabolites were similar between healthy controls and AD cases, while associations with

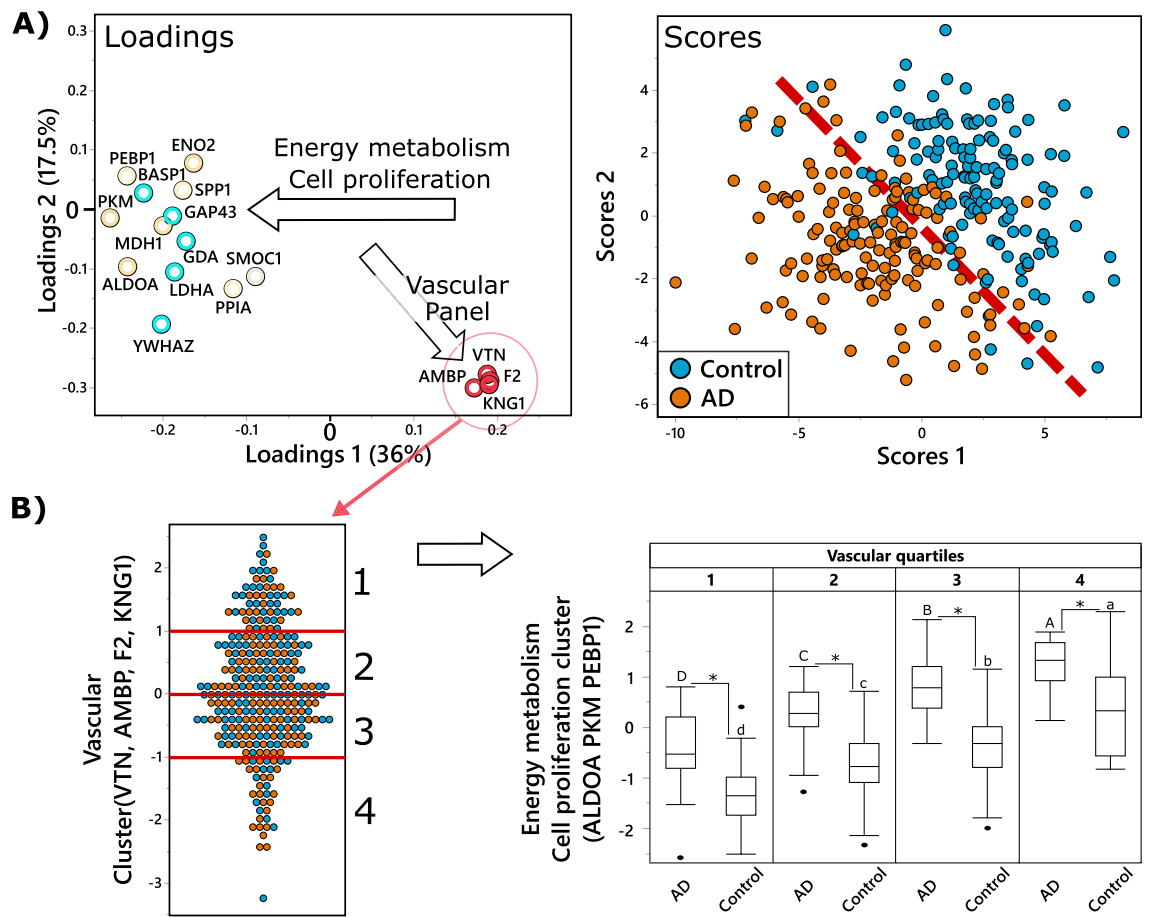


Figure 5. Vascular panel proteins modify relation between energy metabolism-related proteins and AD. **(A)** Partial least square discriminant analysis (PLS-DA) of AD ($n = 151$) vs control ($n = 142$), utilizing CSF proteins. Treatment group discrimination is shown by the SCORES (right panel). The dashed line was added to help show the plain of separation between the two groups, with a plane of discrimination indicated by dashed red line, while metabolites weighting in group discrimination are shown by the LOADINGS (left panel). Proteins in the loading plot are colored based on functional panels, same as in Figs. S2–S5. To facilitate interpretation, arrows on the loading plot indicate directionality, arrow labels indicate the function of discriminating proteins. Analysis was performed with all measured proteins, but only those with variable importance in projection (VIP) ≥ 1 are displayed for clarity. **(B)** Illustration of the relationship between vascular panel proteins (VTN, F2, AMBP, KNG1) and key proteins involved in energy metabolism and cell proliferation (ALDOA, PKM, PEBP1). The panel on the left shows the distribution of the vascular proteins composite score among the subjects, with red lines showing quartiles. The panel on the right shows box and whiskers plots of energy metabolism protein composite score in AD cases and controls, in subjects corresponding to each quartile of the composite score of the vascular panel. Difference in means for each vascular quartile was tested separately for AD cases and healthy controls, using ANOVA with Tukey post-test, with significant differences indicated by capital letters for AD cases and lower letter for the control group. Additionally, differences between AD cases and controls within each vascular quartile was tested using a t-test and significant differences are indicated by an asterisk.

PUFAs were more pronounced in clinical AD. The similarity of observed associations in two independent cohorts of AD cases and healthy controls demonstrates reproducibility of findings and suggests potential importance of the CYP/sEH pathway in healthy CNS.

In plasma, we saw strong positive associations between the LA-derived CYP product (9)10-EpOME, and CSF proteins involved in glycolysis, cell proliferation (PEBP1) and protection from free radicals (SOD1) and negative associations with the CSF vascular panel, including blood coagulation and inflammation proteins. Those associations have opposite directionality than in case of CSF sEH products, consistent with the anti-inflammatory nature of CYP products (epoxy fatty acids) and pro-inflammatory nature of their subsequent sEH metabolites (fatty acids diols)⁴³. Additionally, described associations between plasma (9)10-EpOME, and CSF proteins were only present in AD patients and not in the healthy controls, suggesting the potential involvement of peripheral metabolism in AD pathology. It is important to mention that CYP/sEH pathway is involved in vascular inflammation⁴¹ and potentially could suggest the involvement of dysregulation of the blood brain barrier (BBB). It is plausible that dysregulation of the BBB could open the connection between the periphery and the brain⁴⁴, which would explain AD specific correlation between CSF proteins and plasma, but not CSF metabolites. The disease state specificity of association between inflammation and AD process should be further investigated.

Several studies in animal models for AD and humans have implicated the CYP/sEH pathway in pathogenesis of AD (reviewed in⁴⁵), with a recent study demonstrating upregulation of sEH in the brain of AD cases at the gene and protein level⁴⁶. Our own study identified AD related peripheral and central differences in CYP/sEH metabolism⁷. The CYP/sEH pathway is known for its role in regulation of inflammation^{47,48}, the cardiovascular system⁴⁰, including vascular inflammation⁴¹, ER-stress⁴⁹ and mitochondrial dysfunction⁵⁰. While only correlative, the strong associations of both peripheral and central CYP/sEH metabolites with the CSF vascular protein panel, involved in blood coagulation and cell proliferation are intriguing, providing evidence for peripheral processes to regulate CNS and for synergistic regulation of CYP/sEH pathway in both CNS and periphery. Additionally, our results suggest that the differential levels between healthy and diseased energy metabolism/cell proliferation proteins in the CNS depends on the state of CNS vascular system (lower vascular inflammation and blood coagulation corresponds to higher level of energy metabolism and cell proliferation proteins), providing plausibility for indirect interaction of the CYP/sEH pathway with energy and cell proliferation metabolism. There were previous reports linking the CYP/sEH pathway to energy metabolism in the periphery. In particular, sEH deficiency improves glucose homeostasis⁵¹ and kidney insulin sensitivity⁵² in mouse models, and a sEH polymorphism is associated with insulin sensitivity in type 2 diabetic subjects⁵³. Additionally, sEH inhibition limits mitochondrial damage in a mouse model of ischemic injury⁵⁰. However, to our knowledge, the involvement of the CYP/sEH pathway in CNS energy metabolism was not previously reported. Interestingly, those associations were only observed on metabolite- protein level and not on the gene co-expression level. The disconnect between transcriptomics and proteomics data is well known⁵⁴ as the diversity of regulatory mechanism and regulatory factors increases as we move down the “omics” cascade, further demonstrating the potential and need for integration of metabolomics and proteomics data.

BAs are another group of lipid mediators that showed strong associations with CSF proteins. BAs are known to regulate both inflammation and energy homeostasis through activation of FXR and TGR5 receptors⁵⁵, both abundant in the CNS⁵⁶. Bile acids can cross BBB in two ways, depending on their polarity. Unconjugated bile acids, like DCA or CDCA, can pass through BBB by active diffusion and their plasma levels are highly correlated with the levels in CSF⁵⁶. On the other hand, conjugated bile acids usually require a transporter, resulting in weaker correlations between their levels in plasma and CSF, with some key bile acids like TUDCA and GUDCA manifesting no correlations (the correlation between plasma and CSF metabolites were previously published for this cohort⁷). However, their regulatory function in the CNS is vastly unknown. In our previous work, we have linked brain³⁶ and plasma^{7,35} BAs levels to AD and cognition. Here we observed negative associations between CSF BAs levels and CSF proteins involved in glycolysis and cell proliferation (PEBP1), protection from free radicals (SOD1) and ECM interaction and positive associations with CSF blood coagulation proteins. These associations were formed by both primary and secondary BAs (mainly CDCA and DCA amino acid conjugates), suggesting involvement of liver metabolism as well as of the gut microbiome. Additionally, AD cases showed similar correlative structures to healthy controls, suggesting functionality of the observed correlations beyond AD pathology. Regulation of glycolysis by BAs, through activation of muscle TGR5 receptor was previously reported in mouse models⁵⁷. Also, positive associations of plasma BAs and blood coagulation markers was reported in humans⁵⁸. However, associations of BAs and CNS energy metabolism and regulators of vascular function, to our knowledge have not been previously reported.

In plasma, correlations between BAs and CSF proteins were carried mostly by the ratio of conjugated BAs generated via classic to alternative pathway, suggesting involvement of liver metabolism and by the markers of gut microbiome activity, like the ratio of secondary to primary BAs (DCA/CA). Associations observed here were present only in AD cases and not in healthy controls, suggesting that involvement of peripheral BAs metabolism is dependent on AD case status. Most of the BAs show correlation between plasma and CSF.

In conclusion, this study describes new connection between peripheral and central CYP/sEH and BAs metabolism and CNS energy metabolism, cell proliferation, and vascular function. Additionally, our work highlights the potential of multi-omics data integration and shows the need of further cohort analysis in a multi-omics fashion with matching samples, to enable a more in-depth molecular understanding of AD-associated metabolic perturbations.

Limitations. For plasma, the number of samples for AD patients is different then for the healthy controls. Therefore, apparent differences in associations should be treated with caution and considered only when significant interaction is full factorial model is reported.

Data availability

Metabolomics data is provided by the Alzheimer’s Disease Metabolomics Consortium (ADMC). Metabolomics data and pre-processed data are accessible through the Accelerating Medicines Partnership for AD (AMP-AD) Knowledge Portal (<https://adknowledgeportal.synapse.org/>). The AMP-AD Knowledge Portal is the distribution site for data, analysis results, analytical methodology and research tools generated by the AMP-AD Target Discovery and Preclinical Validation Consortium and multiple Consortia and research programs supported by the National Institute on Aging. Proteomic data and additional information on their generation is available from synapse.org at <https://www.synapse.org/#!/Synapse:syn20821165/wiki/603119>.

Received: 3 March 2023; Accepted: 30 July 2023

Published online: 23 August 2023

References

1. Worheide, M. A. *et al.* Multi-omics integration in biomedical research—A metabolomics-centric review. *Anal. Chim. Acta* **1141**, 144–162 (2021).
2. Clark, C. *et al.* An integrative multi-omics approach reveals new central nervous system pathway alterations in Alzheimer's disease. *Alzheimers Res. Ther.* **13**(1), 71 (2021).
3. Hampel, H. *et al.* Omics sciences for systems biology in Alzheimer's disease: State-of-the-art of the evidence. *Ageing Res. Rev.* **69**, 101346 (2021).
4. Toledo, J. B. *et al.* Metabolic network failures in Alzheimer's disease: A biochemical road map. *Alzheimers Dement.* **13**(9), 965–984 (2017).
5. Barupal, D. K. *et al.* Generation and quality control of lipidomics data for the Alzheimer's disease neuroimaging initiative cohort. *Sci. Data* **5**, 180263 (2018).
6. Kinney, J. W. *et al.* Inflammation as a central mechanism in Alzheimer's disease. *Alzheimers Dement. (N Y)* **4**, 575–590 (2018).
7. Borkowski, K. *et al.* Association of plasma and CSF cytochrome P450, soluble epoxide hydrolase, and ethanolamide metabolism with Alzheimer's disease. *Alzheimers Res. Ther.* **13**(1), 149 (2021).
8. Gabbs, M. *et al.* Advances in our understanding of oxylipins derived from dietary PUFAs. *Adv. Nutr.* **6**(5), 513–540 (2015).
9. Schimke, I. *et al.* Effects of reactive oxygen species on eicosanoid metabolism in human endothelial cells. *Prostaglandins* **43**(3), 281–292 (1992).
10. Bellocchio, L. *et al.* The endocannabinoid system and energy metabolism. *J. Neuroendocrinol.* **20**(6), 850–857 (2008).
11. Chirchiu, V. *et al.* The endocannabinoid system and its therapeutic exploitation in multiple sclerosis: Clues for other neuroinflammatory diseases. *Prog. Neurobiol.* **160**, 82–100 (2018).
12. O'Sullivan, S. E. An update on PPAR activation by cannabinoids. *Br. J. Pharmacol.* **173**(12), 1899–1910 (2016).
13. Zou, S. & Kumar, U. Cannabinoid receptors and the endocannabinoid system: Signaling and function in the central nervous system. *Int. J. Mol. Sci.* **19**(3), 833 (2018).
14. Chiang, J. Y. Bile acid metabolism and signaling. *Compr. Physiol.* **3**(3), 1191–1212 (2013).
15. Shin, D. J. & Wang, L. Bile acid-activated receptors: A review on FXR and other nuclear receptors. *Handb. Exp. Pharmacol.* **256**, 51–72 (2019).
16. Guo, C., Chen, W. D. & Wang, Y. D. TGR5, not only a metabolic regulator. *Front. Physiol.* **7**, 646 (2016).
17. Higginbotham, L. *et al.* Integrated proteomics reveals brain-based cerebrospinal fluid biomarkers in asymptomatic and symptomatic Alzheimer's disease. *Sci. Adv.* **6**(43), 9360 (2020).
18. Goetz, M. E. *et al.* Rationale and design of the Emory healthy aging and Emory healthy brain studies. *Neuroepidemiology* **53**(3–4), 187–200 (2019).
19. Shaw, L. M. *et al.* Cerebrospinal fluid biomarker signature in Alzheimer's disease neuroimaging initiative subjects. *Ann. Neurol.* **65**(4), 403–413 (2009).
20. Hulstaert, F. *et al.* Improved discrimination of AD patients using beta-amyloid(1–42) and tau levels in CSF. *Neurology* **52**(8), 1555–1562 (1999).
21. Pedersen, T. L., Gray, I. J. & Newman, J. W. Plasma and serum oxylipin, endocannabinoid, bile acid, steroid, fatty acid and non-steroidal anti-inflammatory drug quantification in a 96-well plate format. *Anal. Chim. Acta* **1143**, 189–200 (2021).
22. Johnson, E. C. B. *et al.* Large-scale proteomic analysis of Alzheimer's disease brain and cerebrospinal fluid reveals early changes in energy metabolism associated with microglia and astrocyte activation. *Nat. Med.* **26**(5), 769–780 (2020).
23. Benjamini, Y. & Hochberg, Y. Controlling the false discovery rate: A practical and powerful approach to multiple testing. *J. R. Stat. Soc. Ser. B Methodol.* **57**(1), 289–300 (1995).
24. Consortium G.T. The genotype-tissue expression (GTEx) project. *Nat. Genet.* **45**(6), 580–585 (2013).
25. Wan, Y. W. *et al.* Meta-analysis of the Alzheimer's disease human brain transcriptome and functional dissection in mouse models. *Cell Rep.* **32**(2), 107908 (2020).
26. Wörheide, M. A. *et al.* An integrated molecular atlas of Alzheimer's disease. *medRxiv*: 2021.09.14.21263565 (2021).
27. Kuban, W. & Daniel, W. A. Cytochrome P450 expression and regulation in the brain. *Drug Metab. Rev.* **53**(1), 1–29 (2021).
28. McReynolds, C. *et al.* Epoxy fatty acids are promising targets for treatment of pain, cardiovascular disease and other indications characterized by mitochondrial dysfunction, endoplasmic stress and inflammation. *Adv. Exp. Med. Biol.* **1274**, 71–99 (2020).
29. Shearer, G. C. *et al.* Abnormal lipoprotein oxylipins in metabolic syndrome and partial correction by omega-3 fatty acids. *Prostaglandins Leukot. Essent. Fatty Acids* **128**, 1–10 (2018).
30. Lalani, A. I. *et al.* TRAF molecules in inflammation and inflammatory diseases. *Curr. Pharmacol. Rep.* **4**(1), 64–90 (2018).
31. Simpkins, A. N. *et al.* Soluble epoxide inhibition is protective against cerebral ischemia via vascular and neural protection. *Am. J. Pathol.* **174**(6), 2086–2095 (2009).
32. Bazan, N. G., Colangelo, V. & Lukiw, W. J. Prostaglandins and other lipid mediators in Alzheimer's disease. *Prostaglandins Other Lipid Mediat.* **68–69**, 197–210 (2002).
33. Kao, Y. C. *et al.* Lipids and Alzheimer's disease. *Int. J. Mol. Sci.* **21**(4), 1505 (2020).
34. Miyazawa, K. *et al.* Alzheimer's disease and specialized pro-resolving lipid mediators: Do MaR1, RvD1, and NPD1 show promise for prevention and treatment?. *Int. J. Mol. Sci.* **21**(16), 5783 (2020).
35. MahmoudianDehkordi, S. *et al.* Altered bile acid profile associates with cognitive impairment in Alzheimer's disease—An emerging role for gut microbiome. *Alzheimers Dement.* **15**(1), 76–92 (2019).
36. Baloni, P. *et al.* Metabolic network analysis reveals altered bile acid synthesis and metabolism in Alzheimer's disease. *Cell Rep. Med.* **1**(8), 100138 (2020).
37. Ackerman, H. D. & Gerhard, G. S. Bile acids in neurodegenerative disorders. *Front. Aging Neurosci.* **8**, 263 (2016).
38. Ghosh, A. *et al.* Epoxy fatty acid dysregulation and neuroinflammation in Alzheimer's disease is resolved by a soluble epoxide hydrolase inhibitor. *bioRxiv*: 2020.06.30.180984 (2020).
39. Wingo, A. P. *et al.* Integrating human brain proteomes with genome-wide association data implicates new proteins in Alzheimer's disease pathogenesis. *Nat. Genet.* **53**(2), 143–146 (2021).
40. Imig, J. D. Epoxides and soluble epoxide hydrolase in cardiovascular physiology. *Physiol. Rev.* **92**(1), 101–130 (2012).
41. Rajamani, A. *et al.* Oxylipins in triglyceride-rich lipoproteins of dyslipidemic subjects promote endothelial inflammation following a high fat meal. *Sci. Rep.* **9**(1), 8655 (2019).
42. Govindpani, K. *et al.* Vascular dysfunction in Alzheimer's disease: A prelude to the pathological process or a consequence of it?. *J. Clin. Med.* **8**(5), 651 (2019).
43. Deng, Y., Theken, K. N. & Lee, C. R. Cytochrome P450 epoxygenases, soluble epoxide hydrolase, and the regulation of cardiovascular inflammation. *J. Mol. Cell Cardiol.* **48**(2), 331–341 (2010).
44. Sweeney, M. D., Sagare, A. P. & Zlokovic, B. V. Blood–brain barrier breakdown in Alzheimer disease and other neurodegenerative disorders. *Nat. Rev. Neurol.* **14**(3), 133–150 (2018).
45. Hashimoto, K. Role of soluble epoxide hydrolase in metabolism of PUFAs in psychiatric and neurological disorders. *Front. Pharmacol.* **10**, 36 (2019).
46. Ghosh, A. *et al.* Epoxy fatty acid dysregulation and neuroinflammation in Alzheimer's disease is resolved by a soluble epoxide hydrolase inhibitor. *BioRxiv*. <https://doi.org/10.1101/2020.06.30.180984> (2020).

47. Wagner, K. M. *et al.* Soluble epoxide hydrolase as a therapeutic target for pain, inflammatory and neurodegenerative diseases. *Pharmacol. Ther.* **180**, 62–76 (2017).
48. Borkowski, K. *et al.* Walnuts change lipoprotein composition suppressing TNF α -stimulated cytokine production by diabetic adipocyte. *J. Nutr. Biochem.* **68**, 51–58 (2019).
49. Bettaiieb, A. *et al.* Soluble epoxide hydrolase deficiency or inhibition attenuates diet-induced endoplasmic reticulum stress in liver and adipose tissue. *J. Biol. Chem.* **288**(20), 14189–14199 (2013).
50. Akhnokh, M. K. *et al.* Inhibition of soluble epoxide hydrolase limits mitochondrial damage and preserves function following ischemic injury. *Front. Pharmacol.* **7**, 133 (2016).
51. Luria, A. *et al.* Soluble epoxide hydrolase deficiency alters pancreatic islet size and improves glucose homeostasis in a model of insulin resistance. *Proc. Natl. Acad. Sci. USA* **108**(22), 9038–9043 (2011).
52. Luo, J. *et al.* Inhibition of soluble epoxide hydrolase alleviates insulin resistance and hypertension via downregulation of SGLT2 in the mouse kidney. *J. Biol. Chem.* **296**, 100667 (2021).
53. Ohtoshi, K. *et al.* Association of soluble epoxide hydrolase gene polymorphism with insulin resistance in type 2 diabetic patients. *Biochem. Biophys. Res. Commun.* **331**(1), 347–350 (2005).
54. Haider, S. & Pal, R. Integrated analysis of transcriptomic and proteomic data. *Curr. Genomics* **14**(2), 91–110 (2013).
55. Taoka, H. *et al.* Role of bile acids in the regulation of the metabolic pathways. *World J. Diabetes* **7**(13), 260–270 (2016).
56. Mertens, K. L. *et al.* Bile acid signaling pathways from the enterohepatic circulation to the central nervous system. *Front. Neurosci.* **11**, 617 (2017).
57. Sasaki, T. *et al.* Muscle-specific TGR5 overexpression improves glucose clearance in glucose-intolerant mice. *J. Biol. Chem.* **296**, 100131 (2021).
58. Magnusson, M. *et al.* Bile acids and coagulation factors: Paradoxical association in children with chronic liver disease. *Eur. J. Gastroenterol. Hepatol.* **25**(2), 152–158 (2013).

Acknowledgements

All participants from whom plasma and CSF samples were collected provided informed consent under protocols approved by the Institutional Review Board at Emory University. Cohorts included the Emory Healthy Brain Study (IRB00080300), Cognitive Neurology Research (IRB00078273), and Memory @ Emory (IRB00079069). All protocols were reviewed and approved by the Emory University Institutional Review Board. Ethics approval for metabolomics analysis: Analysis samples shipped from Emory was approved for metabolomic profiling and data analysis by the Institutional Review Board at Duke University (Pro00079616). Metabolomics data is provided by the Alzheimer's Disease Metabolomics Consortium (ADMC). The investigators within the ADMC, not listed specifically in this publication's author's list, provided data but did not participate in analysis or writing of this manuscript. A complete listing of ADMC investigators can be found at: <https://sites.duke.edu/admetab/team/>. The Alzheimer's Disease Metabolomics Consortium (ADMC) is funded wholly or in part by the following National Institute on Aging (NIA) grants and supplements, components of the Accelerating Medicines Partnership for AD (AMP-AD) and/or Molecular Mechanisms of the Vascular Etiology of AD (M2OVE-AD): NIA R01AG046171, RF1AG051550, RF1AG057452, R01AG059093, RF1AG058942, U01AG061359, U19AG063744 and FNIH: #DAOU16AMPA awarded to Dr. Kaddurah-Daouk at Duke University in partnership with a large number of academic institutions. Matthias Arnold is further supported by the NIA through grant R01AG069901. Additional support was provided by Emory ADRC P30 AG066511 awarded to Allan I. Levey, Emory EHBS R01 AG070937 awarded to James J. Lah and USDA Intramural Projects 2032-51530-022-00D and 2032-51530-025-00D awarded to John W. Newman. The USDA is an equal opportunity employer and provider.

Author contributions

N.S., J.W.N., A.I.L., K.B. and R.D. designed the study; K.B. and M.A. analyzed data; K.B. wrote the primary manuscript, M.A. and J.W.N. provided comprehensive revision of the manuscript; J.J.L., A.I.L., C.M.H., E.B.D., C.B. and G.L. contributed to data collection, experimental design and they reviewed the manuscript.

Competing interests

Dr. Kaddurah-Daouk is an inventor on a series of patents on use of metabolomics for the diagnosis and treatment of CNS diseases and holds equity in Metabolon Inc., Chymia LLC and PsyProtix, which were not involved in this study. Matthias Arnold is co-inventor (through Duke University/Helmholtz Zentrum München) on patents on applications of metabolomics in diseases of the central nervous system. Matthias Arnold also holds equity in Chymia LLC and IP in PsyProtix and Atai that is unrelated to this work. Kamil Borkowski (through Duke University/UC Davis) is a coinventor on a patent of targeting lipid mediators in Alzheimer's disease. All other authors declare that they have no competing interests.

Additional information

Supplementary Information The online version contains supplementary material available at <https://doi.org/10.1038/s41598-023-39737-8>.

Correspondence and requests for materials should be addressed to K.B. or R.K.-D.

Reprints and permissions information is available at www.nature.com/reprints.

Publisher's note Springer Nature remains neutral with regard to jurisdictional claims in published maps and institutional affiliations.



Open Access This article is licensed under a Creative Commons Attribution 4.0 International License, which permits use, sharing, adaptation, distribution and reproduction in any medium or format, as long as you give appropriate credit to the original author(s) and the source, provide a link to the Creative Commons licence, and indicate if changes were made. The images or other third party material in this article are included in the article's Creative Commons licence, unless indicated otherwise in a credit line to the material. If material is not included in the article's Creative Commons licence and your intended use is not permitted by statutory regulation or exceeds the permitted use, you will need to obtain permission directly from the copyright holder. To view a copy of this licence, visit <http://creativecommons.org/licenses/by/4.0/>.

© The Author(s) 2023